

Effect of Interfacial Chemistry on the Linear Rheology and Thermal Stability of Poly(arylene ether nitrile) Nanocomposite Films Filled with Various Functionalized Graphite Nanoplates

Yingqing Zhan, Fanbin Meng, Xulin Yang, Junji Wei, Jian Yang, Yanke Zou, Heng Guo, Rui Zhao, Xiaobo Liu

Research Branch of Functional Materials, Institute of Microelectronic & Solid State Electronic, High-Temperature Resistant Polymers and Composites Key Laboratory of Sichuan Province, University of Electronic Science and Technology of China, Chengdu 610054, People's Republic of China

Correspondence to: X. Liu (E-mail: liuxb@uestc.edu.cn)

ABSTRACT: Poly(arylene ether nitrile) (PEN) nanocomposites filled with functionalized graphite nanoplates (GNs) were prepared by a simple solution-casting method and then characterized by rheometer and thermogravimetric analysis (TGA). This study investigates how the surface treatment of GNs affects the GN dispersion state. The linear rheological test indicated that the 4-aminophenoxyphthalonitrile-grafted GN (GN-CN) presented better dispersion in PEN matrix than purified GN because the corresponding composite showed the lower rheological percolation threshold, which was further confirmed by scanning electron microscopy and solution experiments. The TGA revealed that the presence of 4-aminophenoxyphthalonitrile-grafted GN retarded the depolymerization evidently compared with that of purified GN, showing remarkable increase in the temperatures corresponding to a weight loss of 5 wt % (increased by 21°C) and maximum rate of decomposition (increased by 9°C). Both the dispersion state and the surface functionalization of GN are very important to the thermal stability of PEN matrix. © 2012 Wiley Periodicals, Inc. *J. Appl. Polym. Sci.* 000: 000–000, 2012

KEYWORDS: poly(arylene ether nitrile); graphite nanoplates; composites; rheology; thermal properties

Received 5 March 2012; accepted 17 April 2012; published online

DOI: 10.1002/app.37903

INTRODUCTION

Poly(arylene ether nitrile) (PEN) is a typical semicrystalline polymer with pendant nitrile groups. As it was first commercialized by Idemitsu in 1986, PEN has attracted attention for high engineering applications, due to their outstanding chemical properties (radiation resistance, low flammability, and toxic gas emission), very good mechanical properties, high heat resistance, high thermal stability, and good molding workability.^{1–3} Furthermore, the cyano group on the aromatic ring appears to promote adhesion of the polymer to many substrates,^{4,5} possibly through polar interaction with other functional groups and it serves as a potential site for polymer crosslinking.^{6–8} Therefore, these properties together with the desired melt processability associated with semicrystalline polymers have resulted in increased interest in using PEN as the matrix for reinforced composites. When graphitic carbons are incorporated, electrically and thermally conductive polymer composites can be produced.^{9,10} Electrically conductive PEN has potential for applica-

tions such as electromagnetic-reflective materials, static charge-dissipative, and electrical coatings.

Graphite nanoplate (GN), a new nanoreinforcement, has attracted tremendous attention in recent years owing to its exceptional physical and chemical properties.^{11–13} One of the most promising applications of this material is in polymer nanocomposites which incorporate nanoscale filler materials. Recent studies showed that this nanomaterial is a potential alternative to clays and carbon nanotubes (CNTs), as it combines the layered structure of clays and the superior thermal and electrical properties of nanotubes.¹⁴ Furthermore, the production cost of GNs is much lower than that of CNTs. Although several cost effective techniques have been developed for the production of GNs, pristine GNs are not compatible with the organic polymer matrix.^{15,16} Therefore, the surface modification of GNs is essential for the production of homogeneously distributed polymer/graphite composite.

© 2012 Wiley Periodicals, Inc.

It is well known that some carbon double bonds were oxidized after the acidic intercalation and thermal treatment, resulting in the presence of oxygen-containing functional groups such as $-\text{COOH}$ and $-\text{OH}$ on the surface of the GNs.¹⁷ Based on the functionality of oxygen, the surface of GNs can be modified in a variety of ways, such as (i) covalent attachment, (ii) noncovalent modification, and (iii) nucleophilic addition.¹⁵ In this study, 4-aminophenoxypthalonitrile was used as an organic modifier to prepare 4-aminophenoxypthalonitrile-grafted GNs (GN-CN), which has been proved to be an effective way to prepare PEN/CNTs composites.¹⁸ Recently, rheometry has been proved to be a powerful tool for investigating the internal microstructure and mesoscopic structure of polymer composites, such as the confinement effect of filler on the motion of polymer chains and the percolated or the flocculated structure of clay tactoids.^{19–21} Rheological responses of polymer/filler nanocomposites are highly dependent on microstructure and mesostructure and particle–particle interactions of filler particles. Therefore, the linear rheological measurements will be necessary to facilitate further insight into the internal structure of polymer/filler system.

Herein, the effect of chemical surface modification of GN on their state of dispersion was examined through rheological and morphological experiments. The objective of the study was to characterize the microstructure of nanocomposites by rheological properties. To further understand the relationship between rheological properties and the state of dispersion of GN, morphological and thermal analyses of PEN/GN nanocomposites were performed.

EXPERIMENTAL

Materials

PEN was provided by Union Laboratory of Special Polymers of UESTC-FEIYA, Chengdu, China. It is a copolymer derived from 2,6-dichlorobenzonitrile with hydroquinone and resorcin with the inherent viscosity of 1.22 dL g^{-1} [0.005 g mL^{-1} in *N*-methylpyrrolidone (NMP)]. GNs were prepared according to the reference reported before.²² The densities of PEN and GN are 1.18 and 2.28 g cm^{-3} , respectively. 4-aminophenoxypthalonitrile were synthesized in our laboratory. Thionyl chloride (99%), were purchased from Kelong reagent, Chengdu, China. All the chemicals and reagents were used without further purification. 4-Aminophenoxypthalonitrile-grafted graphite nanoplates were prepared according to our previous research.²³

Preparation of PEN/GN Nanocomposites

PEN/GN nanocomposites ($\text{PEN}_p\text{GN}_s/\text{PEN}_c\text{GN}_s$, where s denotes the weight ratio of GNs and the lowercase of p and c denotes pure GN and GN-CN, respectively) were prepared by solution-casting method. Typical preparation of PEN/GN-CN was as follows. A certain amount of PEN and 30 mL of NMP were added into a 100-mL three-neck round bottle flask equipped with a mechanical stirrer and refluxing condenser. After the PEN completely dissolved, the GN-CN was dispersed into the PEN solution and refluxed at the stirring speed of 1200 rpm for 3 h, and then sonicated for 3 h in a low-power ultrasonic bath. The mixture was filtered and cast on a clean glass plate. The glass plates were heated at an elevated temperature of

$2^\circ\text{C}\cdot\text{min}^{-1}$ in the oven by the procedure as follows: 80°C , 2 h; 120°C , 2 h; 160, 200°C , 2 h. Finally, the samples were cooled to room temperature gradually, thus, the PEN/GN-CN nanocomposites were obtained. The GN-CN loadings are 0.5, 1, 2, 3, and 5 wt %.

Measurements

Transmission electron microscopy (TEM) was obtained on a JEOL JEM 2010 electro microscope at an accelerating voltage of 200 kV. Samples for TEM analysis were prepared by spreading a drop of a dilute dispersion of the as-prepared products on amorphous carbon-coated copper grids and then dried in air. The morphology of GN and fracture surfaces of the PEN/GN-CN nanocomposites were observed with scanning electron microscope (SEM) (JEOL JSM-5900LV). The SEM samples were coated with a thin layer of gold before examinations.

Dynamical rheological measurements were performed on a rheometer (TA Instruments Rheometer AR-G2) equipped with a parallel-plate geometry (25 mm diameter). The samples with a thickness of 1.0 mm and diameter of 25 mm were melted at 320°C for 5 min in the parallel-plate fixture to eliminate the residual thermal history before measurements. To determine the linear region, the dynamic strain sweep measurements were conducted first. The dynamic frequency sweep measurements were performed in the angular frequency (ω) range of $0.1\text{--}100 \text{ rad s}^{-1}$ at 320°C .

The thermogravimetric analysis (TGA) of the composite was performed under N_2 atmosphere at a heating rate of $20^\circ\text{C min}^{-1}$ using TA Q50 series analyzer system combination with data processing station.

RESULTS AND DISCUSSION

Linear Rheological Behavior of PEN/GN-CN Nanocomposites

Figure 1(a–c) shows the SEM and TEM images of GNs. It can be seen that the diameter of GN is $5\text{--}15 \mu\text{m}$ and the thickness is about 10 nm. After chemically bonded by 4-aminophenoxypthalonitrile, the diameter was slightly decreased [Figure 1(d)]. Most importantly, it can be seen that pure GN has a strong tendency to stack or stamp, whereas GN-CN is quite separated, indicating that the tendency of GN agglomerate after grafting is lowered. Besides, the as-modified GN-CN can be well dispersed in NMP and formed a long-term stable solution [see inset of Figure 1(d)]. This can be attributed to the interaction between strong polar $-\text{CN}$ groups of the grafted GN and solvent molecules. It is believed that grafting of 4-aminophenoxypthalonitrile onto GN would facilitate the preparation of PEN/GN nanocomposites and enhance interfacial affinity between GN and PEN matrix.

Figure 2 shows the development of normalized dynamic storage modulus for PEN_cGN_5 with strain. It can be seen that the region of the linear viscoelastic behavior changed greatly in the presence of the GN-CN. The linear rheological region of the PEN_cGN_s , strain of 1%, was first determined by the dynamic strain sweep. The storage modulus of PEN and PEN composites at 320°C is shown in Figure 3 as a function of frequency. For the entire range of frequency, G' increases with concentration of GN. Neat PEN and composites with low GN incorporation

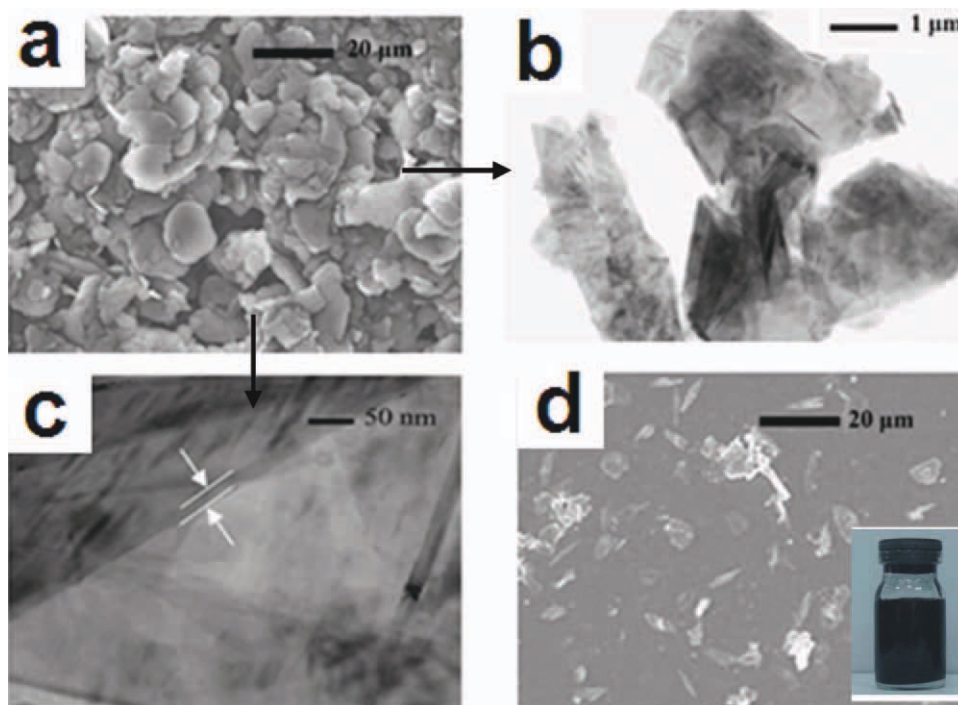


Figure 1. (a) SEM image of GNs, (b) and (c) TEM images of GNs, (d) SEM image of 4-aminophenoxyphthalonitrile grafted GN. Inset of (d) photograph of GN-CN dispersed in NMP. [Color figure can be viewed in the online issue, which is available at wileyonlinelibrary.com.]

display terminal behavior down to lowest test frequency (0.1 rad s^{-1}). With the increase of GN-CN loading, the dependences of G' of PENcGN on ω decrease sharply in the terminal zone, and as can be seen in Figure 3(a), the G' curves exhibit a plateau (at low frequency of $0.1\text{--}1 \text{ rad s}^{-1}$). It indicates that the viscoelastic properties are still dominated by the polymer matrix when the GN-CN loading is low, and PENcGN may experience a transition from liquid-like behavior to solid-like one with the GN-CN loading up to a critical value. Therefore, as shown in Figure 3(b), the low-frequency η^* increases with increasing of GN-CN loading and finally a strong shear-thinning behavior

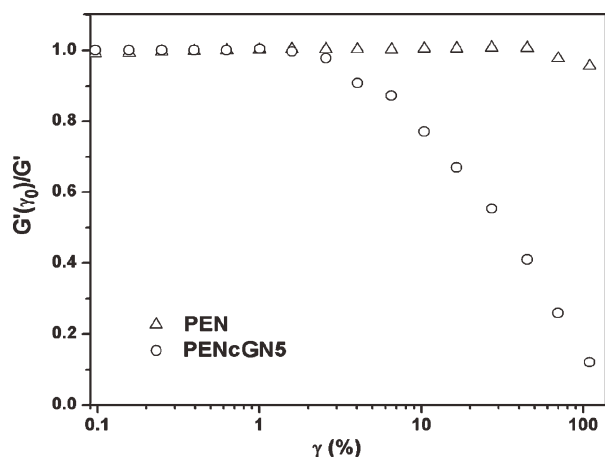


Figure 2. The $G'(\gamma_0)/G'$ for the neat PEN and PENcGN5 samples obtained in the dynamic strain sweep.

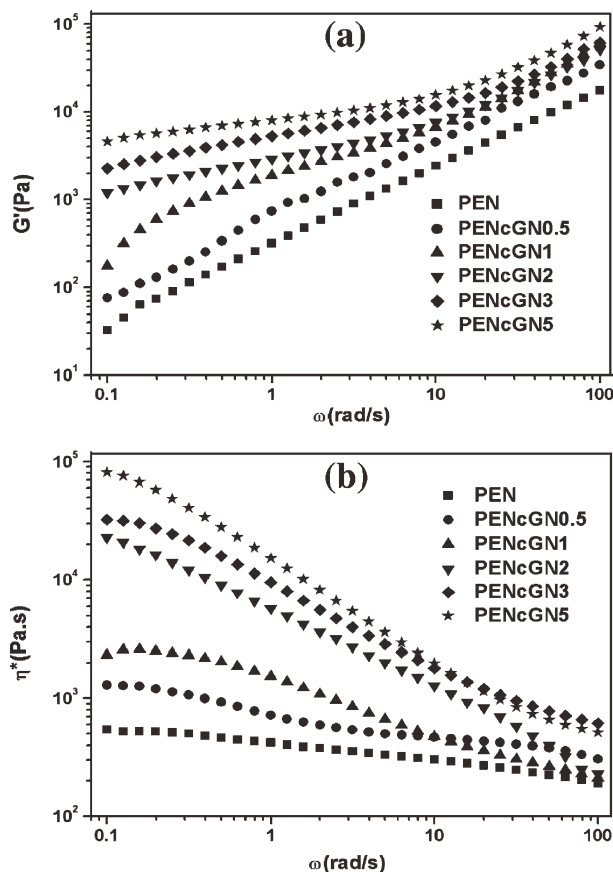


Figure 3. (a) Dynamic storage modulus and (b) complex viscosity for the neat PEN and PENcGNs samples obtained in the dynamic frequency sweep.

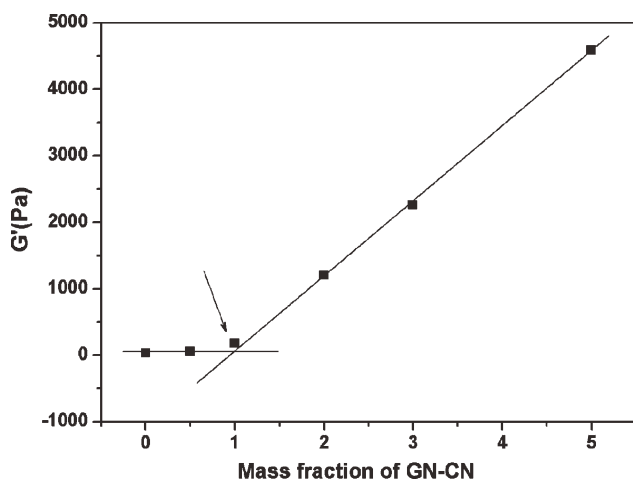


Figure 4. Storage modulus, G' , as a function of the GNs loading at a fixed frequency of 0.1 rad s^{-1} .

appears. The solid-like viscoelastic response results from the formation of transient network as reported by other workers.^{24,25}

To further study the effect of GN-CN loadings on the rheological behavior of PENcGNs, the dependence of the enhancement in low-frequency G' on the GN-CN loadings is probed. Figure 4 shows the low-frequency G' measured at the frequency of 0.1 rad s^{-1} as a function of GN loadings. Compared with that of the PEN matrix, the low-frequency G' of PENcGNs increased by about two orders as the GN-CN loadings achieve up to 2 wt %. This phenomenon can be related to a rheological percolation transition at which the GNs restrict the motion of the polymer matrix. At low GN-CN contents, such filler particles alter the local mobility of individual chains only. At the percolation threshold, these localized restrictions begin to interact across the sample volume, leading to the experimentally observed step change in storage modulus. The elastic modulus of the percolated colloidal suspension can be expressed near the percolation threshold by a power law correlation on the difference between mass fraction of particles m and the threshold value m_{per} ²⁶

$$G' \propto (m - m_{\text{per}})^{\beta}. \quad (1)$$

Assuming the shear modulus of PEN dispersed with GN-CN follows this power law scaling, the percolation threshold m_{per} and exponent β of our system were evaluated by applying Eq. (1) to the G' value at $\omega = 0.1 \text{ rad s}^{-1}$ for GN-CN-reinforced PEN composites. The percolation threshold and exponent calculated from power law correction were 1.2 and 3.72 wt %, respectively. Such low mass fraction at the onset of rigidity percolation and high exponent of GN-CN confirmed that GN-CN is effective in increasing viscoelasticity of PEN. Theoretically, the power law exponent for the rigidity percolation of three-dimensional networks is expected to be greater than 3.^{27,28}

The low percolation threshold of GN is strong evidence for better dispersion. Ren et al.²⁹ showed that a relationship can be constructed between the percolation threshold and the aspect ratio, A_f , of a tactoid. Considering imaginary spheres surround-

ing each tactoid, the expression for the ratio of particle diameter $2r$ to thickness h can be written as

$$A_f = \frac{2r}{h} = \frac{3\phi_{\text{sphere}}}{2\phi_{\text{per}}} \quad (2)$$

Percolation of interpenetrating, randomly packed spheres occurs at $\Phi_{\text{sphere}} = 0.29$.³⁰ To calculate the value of A_f , weight fraction should be converted into volume fraction and densities provided in the experimental part were used ($\rho_{\text{PEN}} = 1.18$ and $\rho_{\text{GN}} = 2.28 \text{ g cm}^{-3}$). Using the onsets of percolation of GN-CN from melt rheology, Eq. (2) gives aspect ratio for GN-CN of 70, which is about four times higher than that of graphite reported previously.³¹

Effect of Functionalization on the Rheological Properties of PEN/GN Nanocomposites

As the linear rheological behavior is very sensitive to the presence of the GNs, the dispersion state of the various GNs could be examined using viscoelastic properties.³² Figure 5(a) gives the dynamic storage modulus (G') and loss modulus (G'') for PEN/GN nanocomposites at identical loading level. At relative lower GN loading of 0.5 wt %, all the samples show higher G'' than G' , indicating that the relaxation is still dominated by the

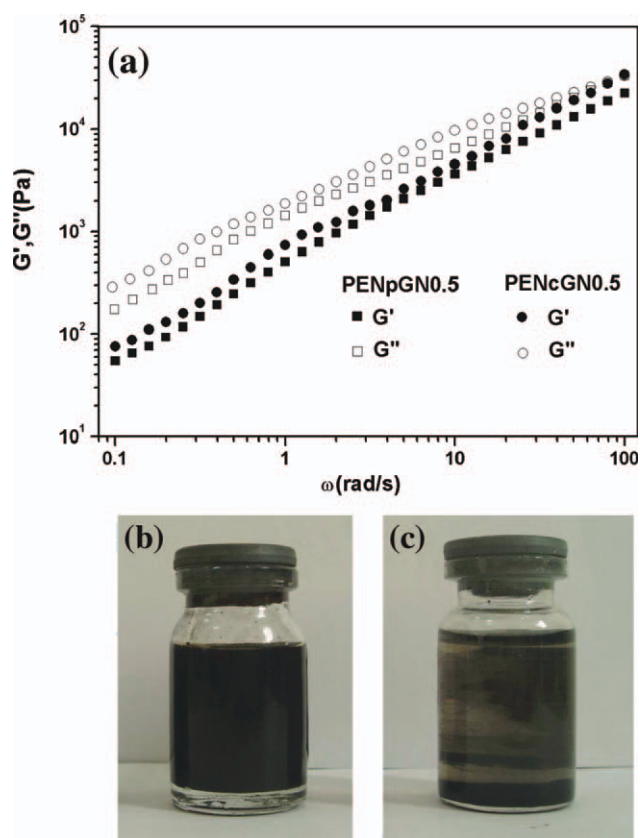


Figure 5. (a) The dynamic storage modulus (G') and loss modulus (G'') for the composite samples with various GN at identical loading level of 0.5 wt %, (b) and (c) photograph of vials, respectively, containing (b) PENcGN0.5 (c) PENpGN0.5 in NMP solution after 8 weeks of their preparation.

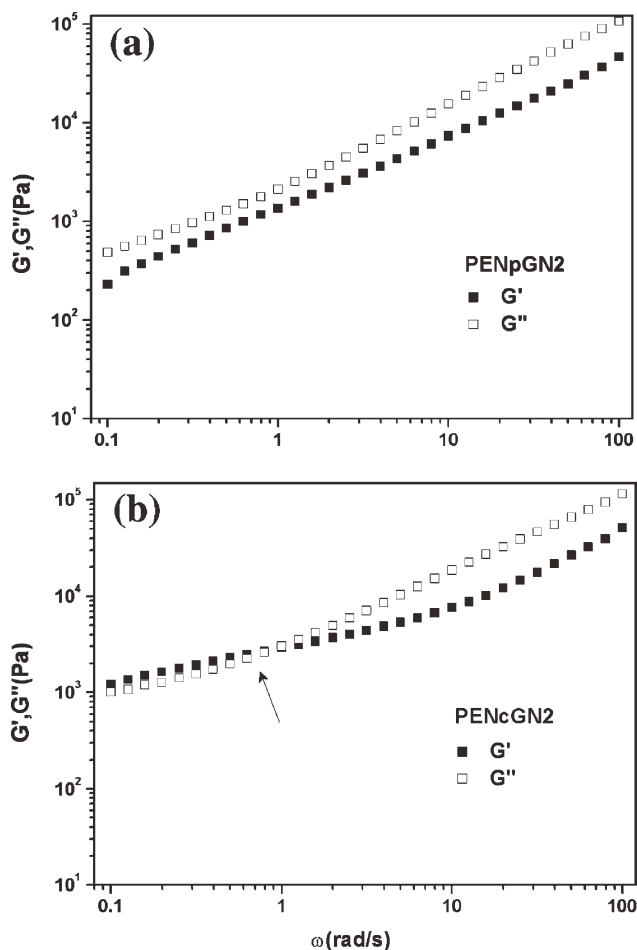


Figure 6. Crossover frequencies between storage and loss modulus for (a) PENpGN2 and (b) PENcGN2.

local PEN dynamics. Thus, the liquid viscoelastic responses were observed on all samples. However, it is notable that the PENcGN0.5 presents higher G'' and G' than that of PENpGN0.5. Because all samples have the identical GN loading, the difference in modulus is an indicative of different dispersion

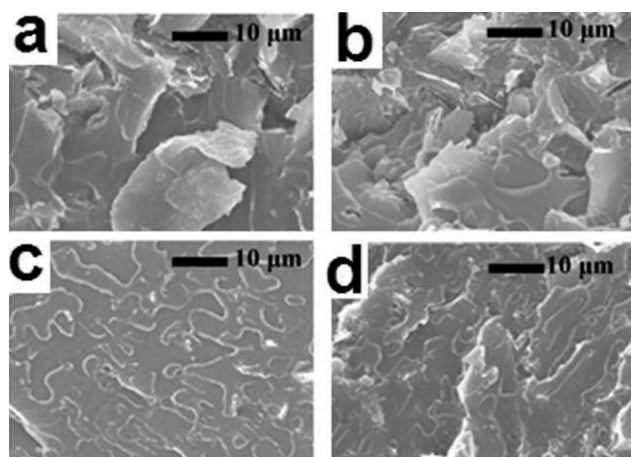


Figure 7. SEM images of (a) PENpGN2, (b) PENpGN5, (c) PENcGN2, and (d) PENcGN5.

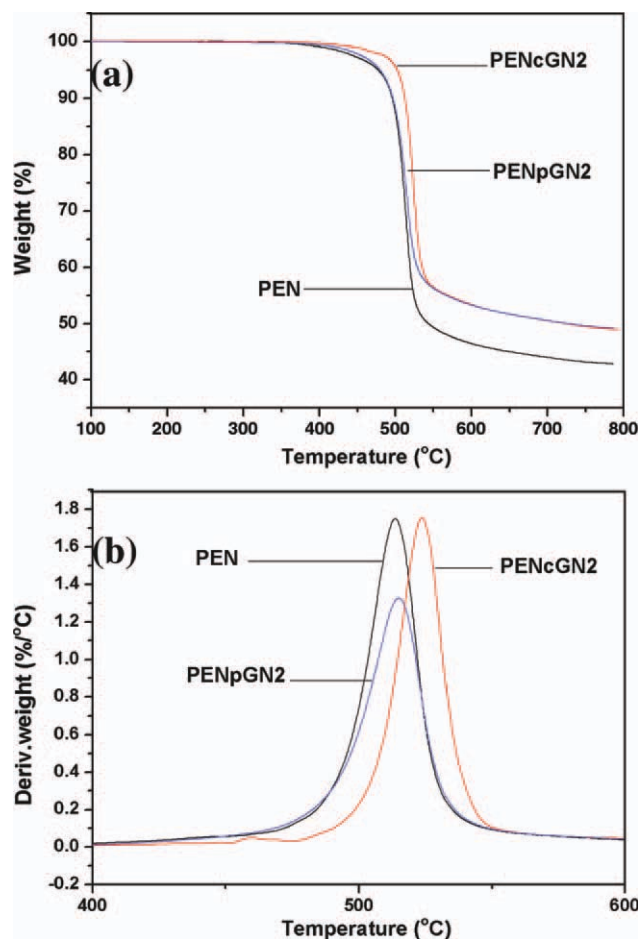


Figure 8. (a) TGA and (b) DTG curves for the neat PEN and its composites with various functionalized GN at identical loading level of 2 wt %. [Color figure can be viewed in the online issue, which is available at wileyonlinelibrary.com.]

state of GN. Therefore, the GN-CN shows the better dispersion in PEN matrix than that of pure GN. This is mainly due to the large difference in affinity between GN and PEN matrix, which is further confirmed by solution experiment.

Figure 5(b,c) shows the photographs of two vials containing equal volumes of solvent (NMP) and equal masses of PEN composites with these two kinds of GNs after 8 weeks of their preparation. It can be seen that PENcGN0.5 sample was completely dissolved in the solvent, forming a dark brown solution without discernable particulate materials and still remains stable for 8 weeks. However, PENpGN0.5 sample cannot be completely dissolved and flocculation is observed. Therefore, in contrast to the purified GN, the presence of strong polar $-\text{CN}$ groups on the functionalized GN enhances the affinity between the GN and PEN matrix, promoting the diffusion of polymer chain into the aggregates of GN effectively.

Figure 6 shows the dynamic storage modulus (G') and loss modulus (G'') for PEN/GN nanocomposites at identical loading level of 2 wt %. Lele et al.³³ described solid-like and liquid-like behavior by means of storage and loss modulus. The solid-like behavior is characterized as not only the storage modulus

Table I. Thermal Properties of Neat PEN and PEN Its Composites with Various Functionalized GN at Identical Loading Level of 2 wt %

Sample	T_5 wt % ^a (°C)	T_{max} ^b (°C)	Char yield at 800°C (wt %)
PEN	478	515	42.8
PENpGN2	483	516	49.1
PENcGN2	499	524	48.9

^a T_5 wt %—temperature corresponding to a weight loss of 5 wt %, ^b T_{max} —temperature corresponding to maximum rate of decomposition.

higher than the loss modulus but also lower crossover frequency. As shown in Figure 6(a), the PENpCN2 sample does not denote the crossover point, whereas PENcGN2 sample has the crossover points. This indicates that —CN-treated GN nanocomposite is a percolated system and shows more solid-like behavior than PENpGN2. Therefore, it is reasonable to propose that 4-aminophenoxyphthalonitrile-grafted GN shows better dispersion in the PEN matrix than that of pure GNs, which is further confirmed by SEM measurements. Figure 7 shows the SEM images of PENcGN and PENpGN samples with various GN loadings. Clearly, pure GNs are aggregated seriously, showing very poor dispersion in the PENpGN2 and PENpGN5 [Figure 7(a,b)]. Compared with the PENpCN samples, PENcGN2 and PENcGN5 present better dispersion of functionalized GN. Besides, some GNs are pulled out from the polymer matrix in the PENpGN2 and PENpGN5 [Figure 7(c,d)] samples. These results indicate that the 4-aminophenoxyphthalonitrile-grafted GN may have better affinity with PEN chain than that of purified GN.

Thermal Properties of PEN/GN Nanocomposites

It is generally believed that the introduction of inorganic components into organic materials can improve their thermal stabilities.^{34,35} Addition of GN increases the temperature corresponding to a weight loss of 5 wt % (T_5 wt %) and/or to the onset decomposition by about 10–20°C or even more. This improvement is mainly attributed to good matrix–nanoplates interaction, thermal conductivity of the nanosheets, and also due to their barrier effect. The results from the thermal analysis of the PEN/GN nanocomposites were shown in Figure 8 and summarized in Table I. Clearly, the PENpGN2 and PENcGN2 present the similar thermal stable residue, which corresponded well with the GN loadings. Compared with that of the neat PEN, remarkable improvement in T_5 wt % is observed in the PEN composites, as shown in Table I. This indicates that the addition of GNs efficiently improves the thermal stability of the PEN. As for the PEN composites with functionalized GN, it can be seen that the composite with GN-CN shows outstanding higher T_5 wt % than that of pure GNs. This is attributed to relatively better dispersion of the GN-CN than that of pure GNs, in agreement with the SEM and dissolution experiment discussion.

With increase in the decomposition level, the thermal conductive and barrier effects of the GN become more effectual. Figure 8(b) shows the DTG curves and the temperatures corresponding to the maximum rate of decomposition (T_{max}). It can be seen that the

PENpGN sample shows the similar T_{max} compared to that of neat PEN. However, it is very interesting that T_{max} of PENcGN2 samples increases by 9°C, compared with that of neat PEN. Two possible mechanisms were proposed to explain this phenomenon. On the one hand, the good dispersion highly enhances the barrier effects of GN-CN, and percolation network may also enhance their thermal conductive efficiency. In this case, the dispersion state becomes dominant and the T_{max} of PENcGN2 increases evidently as a result. Conversely, due to the nitrile group (—CN) grafted on the surface of the GNs, the crosslinking reaction of nitriles group between GN-CN and polymer matrix would happen, which further enhances the thermal stability of PEN composite.

CONCLUSIONS

In this study, the PEN nanocomposites with functionalized GN were prepared through solution-casting method and investigated for morphological, rheological, and thermal properties. The rheological test shows that PEN/GN-CN nanocomposites present a typical solid-like viscoelastic response at low frequencies, and the percolation is lower than 2 wt %. The surface functionalization influences the dispersion state of GN in the PEN matrix strongly. The GN-CN shows the relatively better dispersion than pure GN. Because of good affinity between nitriles group and PEN matrix, 4-aminophenoxyphthalonitrile-grafted GN retarded the depolymerization evidently compared with that of pure GN.

ACKNOWLEDGMENTS

This work was financially supported by the Fundamental Research Funds for the Central Universities (E022050205), Major Science and Technology Project in Sichuan Province (2010 FZ 0117) “863” National Major Program of High Technology of China (No. 2012AA03A212), and National Natural Science Foundation (No. 51173021).

REFERENCES

- Saxena, A.; Sadhana, R.; Rao, V. L.; Kanakavel, M.; Ninan, K. N. *Polym. Bull.* **2003**, *50*, 219.
- Takahashi, T.; Kato, H.; Ma, S. P.; Sasaki, T.; Sakurai, K. *Polymer* **1995**, *36*, 3803.
- Zhan, Y. Q.; Yang, X. L.; Meng, F. B.; Lei, Y. J.; Zhong, J. C.; Zhao, R.; Liu, X. B. *Polym. Int.* **2011**, *60*, 1342.
- Verborgt, J.; Marvel C. S. *J. Polym. Sci. Polym. Chem. Ed.* **1973**, *11*, 2793.
- Sivaramakrishnan, K. V.; Marvel, C. S. *J. Polym. Sci. Polym. Chem. Ed.* **1974**, *12*, 651.
- Anderson, R. R.; Holvoka, J. M. *J. Polym. Sci.* **1966**, *4*, 1689.
- Keller, T. M. *J. Polym. Sci. Polym. Chem.* **1988**, *26*, 3199.
- Keller, T. M. *Polymer* **1993**, *34*, 952.
- Kim, H.; Abdala, A. A.; Macosko, C. W. *Macromolecules* **2010**, *43*, 6515.
- Zhan, Y. Q.; Lei, Y. J.; Meng, F. B.; Zhong, J. C.; Zhao, R.; Liu, X. B. *J. Mater. Sci.* **2011**, *46*, 824.

11. Park, J. K.; Dob, I. H.; Askeland, P.; Drzal, L. T. *Compos. Sci. Technol.* **2008**, *68*, 1734.
12. Rath, T.; Li, Y. J. *Composites A* **2011**, *42*, 1995.
13. Lau, S. T.; Chan, L. H.; *J. Appl. Polym. Sci.* **2011**, *119*, 1166.
14. Kalaitzidou, K.; Fukushima, H.; Drzal, L. T. *Carbon* **2007**, *45*, 1446.
15. Dreyer, R. D.; Park, S.; Bielawski, C. W.; Ruoff, R. S. *Chem. Soc. Rev.* **2010**, *39*, 228.
16. Kuila, T.; Bhadra, S.; Yao, D.; Kim, N. H.; Bose, S.; Lee, J. H. *Prog. Polym. Sci.* **2010**, *35*, 1350.
17. Che, R. C.; Peng, L. M.; Duan, X. F.; Chen, Q.; Liang, X. L. *Adv. Mater.* **2004**, *16*, 401.
18. Zhong, J. C.; Jia, K.; Lei, Y. J.; Liu, X. B. *Int. J. Mater. Eng. Technol.* **2010**, *3*, 53.
19. Zhang, M. Q.; Lin, B.; Sundararaj, U. *J. Appl. Polym. Sci.* **2012**, *125*, E714.
20. Krishnamoorti, R.; Vaia, R. A.; Giannelis, E. P. *Chem. Mater.* **1996**, *8*, 1728.
21. Solomon, M. J.; Almusallam, A. S.; Seefeldt, K. F.; Varadan, P. *Macromolecules* **2001**, *34*, 1864.
22. He, F.; Lau, S.; Chan, H. L.; Fan, J. T. *Adv. Mater.* **2009**, *21*, 710.
23. Zhan, Y. Q.; Yang, X. L.; Meng, F. B.; Wei, J. J.; Zhao, R.; Liu, X. B. *J. Colloid Interface Sci.* **2011**, *363*, 98.
24. Botta, L.; La Mantia, F. P.; Dintcheva, N. T.; Scaffaro, R. *Macromol. Chem. Phys.* **2007**, *208*, 2533.
25. Song, Y. S. *Polym. Eng. Sci.* **2006**, *46*, 1350.
26. Du, F. M.; Scogna, R. C.; Zhou, W.; Brand, S.; Fischer, J. E.; Winey, K. I. *Macromolecules* **2004**, *37*, 9048.
27. Kanai, H.; Navarrete, R. C.; Macosko, C. W.; Scriven, L. E. *Rheol. Acta* **1992**, *31*, 333.
28. Feng, S.; Sen, P. N. *Phys. Rev. Lett.* **1984**, *52*, 216.
29. Ren, J.; Silva, A. S.; Krishnamoorti, R. *Macromolecules* **2000**, *33*, 3739.
30. Balberg, I. *Phys. Rev. B* **1985**, *31*, 4053.
31. Kim, H.; Macosko, C. W. *Macromolecules* **2008**, *41*, 3317.
32. Wu, D. F.; Zhang, M.; Zhao, Y. L. *Polym. Degrad. Stab.* **2008**, *93*, 1577.
33. Lele, A.; Mackley, M.; Galgali, G.; Ramesh, C. *J. Rheol.* **2002**, *46*, 1091.
34. Li, M. L.; Jeong, Y.; G. *J. Appl. Polym. Sci.* **2012**, *125*, E532.
35. Kim, H. S.; Park, B. H.; Yoon, J. S.; Jin, H. J. *Eur. Polym. J.* **2007**, *43*, 1729.